



## Considerations for Choosing an Alpha Spectroscopy PIPS Detector

### PIPS® DETECTORS

#### General Characteristics

Alpha spectroscopy demands reliable, rugged and stable charged particle detectors having low noise, good resolution and high efficiency. With 25 years of Silicon detector manufacturing, proprietary processes, and device designs, the Canberra™ PIPS detectors successfully meet all these requirements. The success of Passivated Implanted Planar Silicon (PIPS) detectors is enabled by using industry standard silicon processing techniques. Over the years we have delivered around 100 000 PIPS detectors.



Salient features of PIPS technology include the following:

- Buried Ion Implanted Junctions
- SiO<sub>2</sub> Passivation
- Low Leakage Current
- Low Noise
- Thin windows (< 500 Å eq. Si.)
- Ruggedness (cleanable surface)
- Bakeable at High Temperatures (100 °C)



#### Operating Principle

In the detection process, particles are stopped in the depletion region, forming electron-hole pairs. The energy necessary to form a single electron-hole pair depends on the detector material, but is essentially independent of the energy of the incoming particle. The number of electron-hole pairs ultimately formed is thus directly proportional to the energy of the particle. The electric field in the depletion region sweeps the electrons to one terminal and the holes to the other. The resultant charge pulse is integrated in a charge sensitive preamplifier to produce a voltage pulse.

$$N = E/\epsilon$$

E represents the kinetic energy of the particle and  $\epsilon$  the energy necessary to create one ion-electron pair.  
 $\epsilon = 3.61$  eV for Silicon.

The thickness of the depletion region depends upon the applied bias voltage, so that higher voltages give a thicker region, capable of stopping more energetic particles.

The capacitance (in pF) of the detector is given by

$$C = \frac{1.05 A}{W}$$

where A (in cm<sup>2</sup>) represents the surface of the junction. It is typically 20% higher than the active area of the detector.

W (in cm) represents the thickness of the detector and is given by:

$$W = 0.562 \sqrt{\rho V}$$

V is the applied bias in Volts and  $\rho$  the resistance in ohm-cm. It is thus possible to have a partially depleted or a fully depleted detector with and without overvoltage as illustrated in Figure 1.

The noise level of charge-sensitive preamplifiers is usually given by the manufacturer as a certain value for zero input capacitance. The noise level increases with capacitance and this rate of increase is also specified. The detector capacitance is reduced at higher voltages, so that the lowest noise and best resolution are obtained at higher voltages within the recommended range. At voltages above that recommended by the manufacturer, the reverse leakage current will likely increase, causing excessive noise and a loss of resolution.

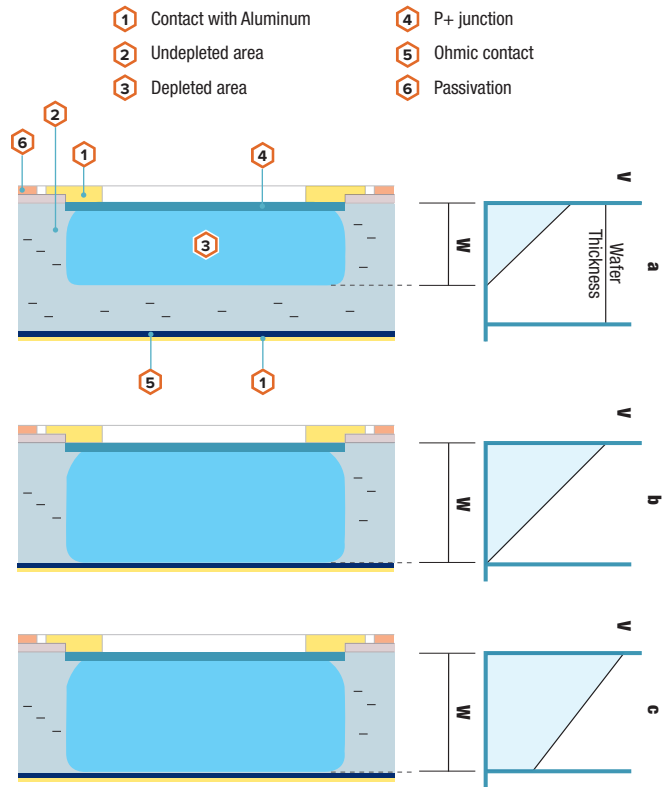


**Figure 1**  
 Thickness W of the depletion layer as a function of applied bias  
 a. partially depleted mode  
 b. fully depleted mode  
 c. fully depleted mode with overvoltage

## The A Series PIPS Detectors

### Key Properties and Applications

The A Series PIPS Detectors are optimized for Alpha particle detection or Alpha Spectroscopy applications which require high resolution, high sensitivity and low background.

In order to ensure high resolution, energy straggling has to be minimized. Energy straggling is due to the random nature of the interaction of a charged particle with the detector material. This leads to a spread in energy if a beam of charged particles passes through a certain thickness of absorber and, consequently results in an increase of the peak width. High resolution is ensured by the thin entrance window over the detector surface. It reduces energy straggling in the entrance window. Furthermore, the low leakage current ensures a low electronic noise contribution. Both properties together allow a high resolution. Values  $\leq 16$  keV (FWHM) are routinely achieved for a detector with an active area of 450 mm<sup>2</sup>.

High sensitivity is enhanced by good resolution, which reduces the background below the peak.

Absolute efficiency of up to 40% can be achieved.

Low background is achieved through the use of carefully selected packaging materials and through clean manufacturing and testing procedures.

Backgrounds of less than 0.05 cts/hr cm<sup>2</sup> are routinely achieved.

The A series PIPS find applications in widely different scientific disciplines such as:

- radiochemical analysis
- environmental studies and surveys
- health physics
- survey of nuclear sites through the off-line detection of emitted actinides
- geological and geomorphological studies (such as U-Th dating etc.)

Note however that the obtainable resolution depends not only on the detector, but also on external factors such as source preparation, operating pressure, source-detector distance, and especially preamplifier and/or spectrometer quality. At lower bias voltages and resistivities, the detectors are partially depleted. Alpha PIPS detectors have a minimum depletion depth of 140 microns. This is enough to absorb a particles of up to 15 MeV covering the complete range of all alpha-emitting radionuclides (Appendix 1).

Table 1 shows the detector specifications and operating characteristics for the A Series PIPS detectors.

Table 1					
MODEL	A300	A450	A600	A900	A1200
Active Area (mm <sup>2</sup> )	300	450	600	900	1200
Active Diameter (mm)	19.5	23.9	27.6	33.9	39.1
Thickness (min/max $\mu$ m)	150/315				
Bias (min/max V)	+20/100				
Bias (recommended V)	+20/80				
Si-Resistivity (min ohm-cm)	2000				
Operation Temp. (min/max $^{\circ}$ C)	-20/+40				
Storage Temp. (max $^{\circ}$ C)	+100				
Leakage current (typ/max) nanoamps at 25 $^{\circ}$ C <sup>1</sup>	35/70	50/100	60/120	100/200	150/300
Alpha Resolution <sup>2</sup> keV (FWHM)	17	18	22	25	32
Absolute Efficiency (%) <sup>3</sup>					
at 2 mm spacing	37	40	42	44	45
at 5 mm spacing	24	28	31	35	37
at 15 mm spacing	7	11	12	16	19

1) These values are 5 to 10 times smaller than those of corresponding surface barrier detectors.  
 2) For the 5.486 MeV Alpha line of <sup>241</sup>Am at 15 mm Detector-Source spacing using standard Mirion electronics. Detectors are not tested with an alpha source in order to avoid low level contamination. Beta resolution is typically 5 keV less than Alpha resolution and is approximated by pulser line width.  
 3) With a source diameter of 15 mm.

## Factors Influencing Resolution and Efficiency

### Detector-Source Distance

All Alpha particles reaching the active surface of an A-series detector will be counted. The counting efficiency is thus given by the geometrical efficiency  $N = \Omega/4\pi$ .

Where  $\Omega$  is the solid angle under which the detector subtends the source. For the case of a circular detector coaxial to a circular isotropic source disc, this solid angle can be computed by Monte-Carlo calculations<sup>1</sup> and is available in tabulated form<sup>2</sup>.

Figures 2, 3, 4 and 5 give Alpha efficiencies based on such solid angle evaluations and experimental verifications (expressed in % of the total emitted Alpha particles for various detectors as a function of source to detector distance for 3 different ideal sources with diameter of 15, 25 and 32 mm). Actual efficiencies may be slightly different, especially at small source detector distances, due to factors such as self absorption in the source, etc. Efficiencies of up to about 40% are obtainable.

When the source approaches the detector, line broadening (FWHM) is expected, as the mean slope of the alpha particles entering the detector is increased, resulting in an effectively increased thickness of the entrance window and subsequent higher energy straggling<sup>3</sup>. For Alpha PIPS this energy straggling is minimized due to the very thin entrance window of 500 Å. Figure 6 shows the experimental mean percent variation of the resolution for a 300 to 600 mm<sup>2</sup> detector as a function of the source detector distance, h.

It is seen that even for values of h as small as 2 mm, the increase of the peak width stays below 50%.

For a model A300-17 AM detector the alpha resolution at 3 mm source to detector distance is thus expected to be:  $R = 17(1+0.41) = 25 \text{ keV (FWHM)}$ .

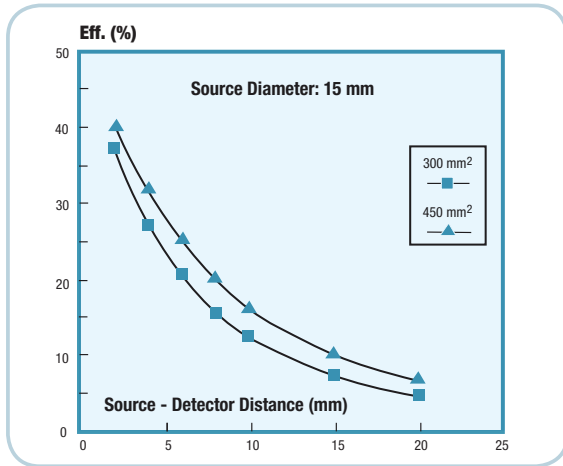


**Figure 2**

Geometric efficiency as a function of source-detector distance for a circular 15 mm diameter source coaxial with the detector.

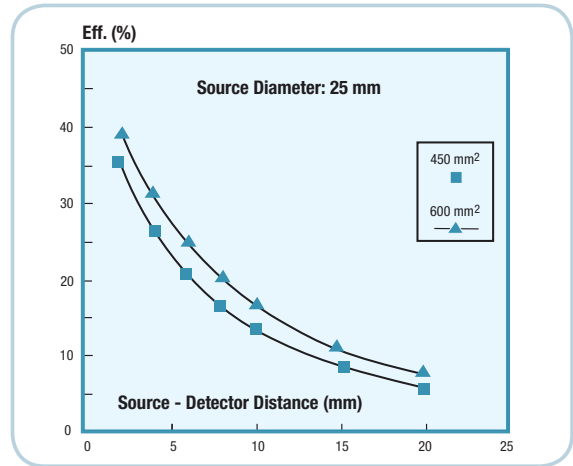


**Figure 3**

Geometric efficiency as a function of source-detector distance for a circular 25 mm diameter source coaxial with the detector.

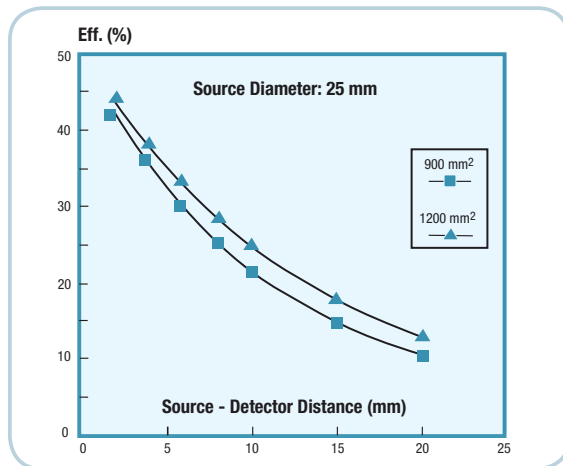


**Figure 4**

Geometric efficiency as a function of source-detector distance for a circular 25 mm diameter source coaxial with the detector.

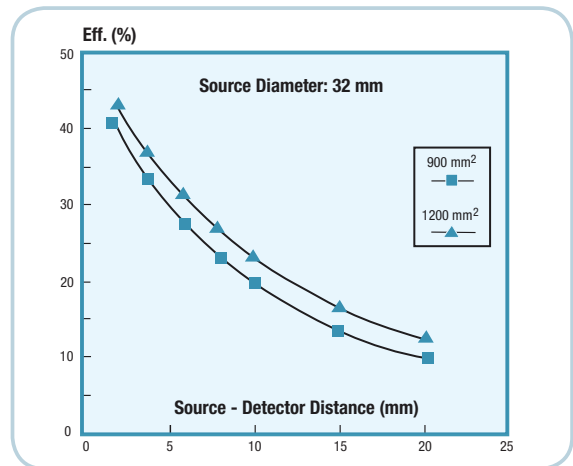


**Figure 5**

Geometric efficiency as a function of source-detector distance for a circular 32 mm diameter source coaxial with the detector.

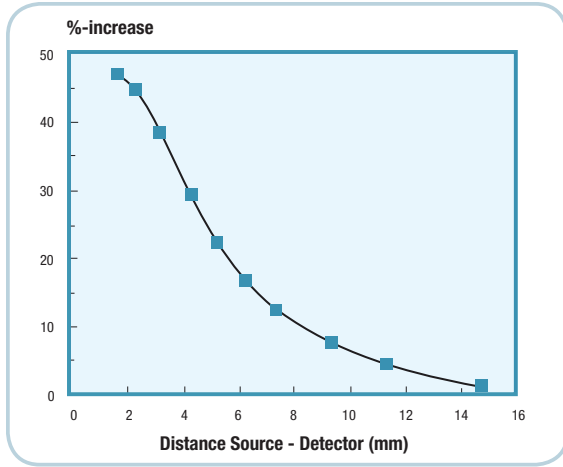


**Figure 6**  
Empirical mean percent increase of peak line width.  
Source diameter: 15 mm  
Detector area: 300 to 600 mm<sup>2</sup>

### Source Radius

It is interesting to take a closer look at the influence of the source diameter on the efficiency. Figure 7 shows the geometrical efficiency of a 450 mm<sup>2</sup> and a 1700 mm<sup>2</sup> detector as a function of the source radius for a source to detector distance of 5 mm. One sees immediately that the efficiency of the bigger detector is much greater, whatever source radius is chosen. Note, however, the existence of an inflection point for  $R_s = R_d$  as well as the sharp decrease in efficiency beyond this point.

$R_s$  and  $R_d$  represent the source and detector radii. The diameter of the source should thus never exceed the diameter of the detector. If a uniform specific source activity  $A_s$  (Bq/cm<sup>2</sup>) is assumed, the total number of counts registered in a time  $t$  is proportional not only to the efficiency but also to the total activity of the source deposited on the surface area or, in other words, the efficiency multiplied by the Activity  $A_s$ . Figure 8 gives this number as a function of the source radius in arbitrary units.

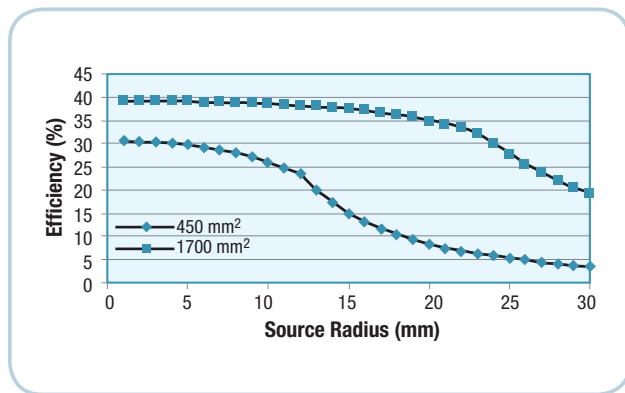


**Figure 7**  
Geometrical efficiency of a 1700 mm<sup>2</sup> (upper curve) and a 450 mm<sup>2</sup> (lower curve) a-detector as a function of the source diameter given in mm for a source detector distance of 5 mm<sup>2</sup>

Note that when the source radius exceeds that of the detector, the gain in source surface is exactly compensated by the loss in efficiency. The optimum source radius thus equals the radius of the detector. This general rule is independent of the source to detector distance.

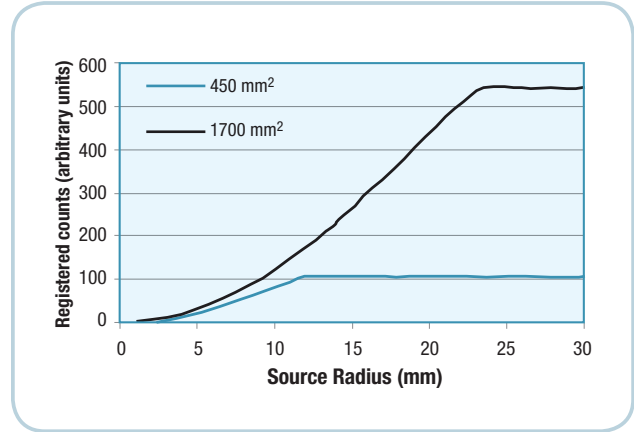


**Figure 8**  
Number of counts registered during a certain time  $Dt$  (arbitrary units) for a 1700 mm<sup>2</sup> and a 450 mm<sup>2</sup> detector as function of the source radius in mm

### Source Thickness

Sources must be homogeneous and thin in order to avoid energy straggling due to self-absorption<sup>4</sup>. Self-absorption is proportional to the thickness of the source and inversely proportional to the specific activity. For typical values of specific activities in the order of 100 Bq/cm<sup>2</sup>, the self-absorption is generally negligible for carrier-free sources. Note, however, that the thickness of the carrier-free source depends on the transition probability of the isotope in question and thus increases with increasing half-life. Expressed in energy loss, it is on the order of 0.03 keV for “short” lived isotopes such as <sup>239</sup>Pu (2.4 x 10<sup>4</sup> y) and <sup>230</sup>Th (7.5 x 10<sup>4</sup> y), while for “long” lived isotopes such as <sup>238</sup>U (4.7 x 10<sup>9</sup> y) it is on the order of 5 keV.

When estimating the source thickness of a non carrier-free source, all isotopes deposited together with the isotope of interest must be considered. This can be due either to a different isotope of the same element or to the simultaneous deposition of other elements during source preparation.

Problems can also arise with very intense sources as self-absorption is proportional to the total source activity. For a same total activity the specific activity can be reduced by choosing a larger source diameter. In this case, preference should be given to a detector with a diameter about equal to that of the source in order to increase its efficiency (Figure 2) and to reduce the energy straggling as fewer Alpha particles will strike the detector at an acute angle.

---

## Factors Influencing Contamination and Stability

### Oil Contamination

Typical Alpha Spectroscopy Systems use a rotary vane vacuum pump to evacuate the Alpha Spectrometer(s). When static conditions are established in the vacuum system (the ultimate pressure has been reached) and there is no substantial gas flow towards the pump, oil particles can back-stream towards the spectrometer and deposit on the detector and the source surfaces. The same can happen in a more dramatic fashion if the pump is disabled and the spectrometer draws air backwards through the manifold connecting the two.

For this reason it is recommended that a backstreaming filter be used between the pump and the plumbing to the spectrometer or that a dry pump be used instead to prevent oil contamination.

### Particulate and Recoil Contamination

Contamination of detectors can take place when particles from sources gravitate to the detector surface and stick there or are splattered, sputtered, or splashed on the detector surface by the recoil energy imparted to the nucleus of an Alpha-emitting atom. In the latter case the energy of the particulates may be sufficient to implant them in the detector so that they can only be removed destructively.

Much of the casual contamination can be removed from PIPS detectors by cleaning with a swab saturated with isopropanol. Vigorous scrubbing will not harm the PIPS detector.

Recoil contamination is almost never 100% removable so it is best avoided by careful sample preparation, avoiding hot samples, or by using the techniques reported by Sill & Olsen<sup>5</sup> which involve operating the spectrometer with an air barrier and a bias voltage between detector and source. They show that recoil contamination can be reduced by a factor of up to 1000 if an air layer of about 12 mg/cm<sup>2</sup> exists between the detector and source and if the source is biased negatively by a few volts. The air gap will increase the width of alpha peaks by a few keV which is probably acceptable in all but the most demanding of applications.

The Mirion Alpha Spectrometers and Accessories are available with sample bias, pressure control, and monitoring capability.

### Stability

Both long-term and temperature stability are important in detectors used for Alpha Spectroscopy because count times are often many hours or days and gain shifts during data accumulation lead to erroneous or unusable spectra.

### Long Term Stability

The long-term stability is affected by the impact of the environment on detector junctions. Silicon surface barrier (SSB) detectors sometimes fail with prolonged exposure to room atmosphere and at other times they fail when operated for prolonged periods under high vacuum. This instability is caused by the epoxy edge encapsulation that is required for this type of detector. The PIPS detector has junctions that are buried in the silicon bulk. No epoxy encapsulation is needed or used so the PIPS detector has intrinsic long-term stability.

### Temperature Stability

The leakage current of silicon diodes doubles for every 5.5 to 7.5 °C change in ambient temperature. Since the preamp H.V. bias resistor is a noise contributor, it is necessarily of high value, typically 100 megohm. With a SSB detector having leakage current of 0.5 µA, the change in bias voltage at the detector for a 2 °C change in ambient temperature can be as much as 13 V. This is enough bias change to affect overall gain of the detector preamplifier by a substantial amount.

PIPS detector has a low leakage current, consequently no significant changes in resolution are observed up to operational temperatures above 35 °C.

## The Minimum Detectable Activity MDA

### For Single Radionuclide Samples

The minimum detectable activity (MDA) is a measure of the lowest level at which sample activity can be distinguished from background. For a 95% confidence limit it is given by<sup>6</sup>:

$$MDA \text{ (Bq)} = \frac{2.71 + 4.65 \sqrt{b}}{t N P}$$

t = counting time

N = counting efficiency

P = yield of the Alpha in question

b = background counts

The two detector-bound parameters, background (b) and the efficiency (N) are particularly favorable in the case of an Alpha PIPS detector as seen from Table 1 and Figures 2-5. For a 450 mm<sup>2</sup> detector (N = 0.40, b = 6 cts/day) and an overnight run (t = 15 hr = 54 000 s) one has:

$$MDA = 0.54 \text{ mBq} \\ \text{(100\% yield is assumed.)}$$

This is a worst case condition which assumes that all the background counts are in the peak or region of interest.

The choice of a particular detector will be governed very often by this MDA. However, as seen earlier, the limiting factor will very often not be the absolute MDA expressed in Bq, but rather the specific minimum detectable activity SMDA expressed in Bq/cm<sup>2</sup>:

$$SMDA = \frac{MDA}{A(s)}$$

Where  $A(s)$  represents the area of the source. In the case where the source area equals the detector area Figure 9 gives this SMDA in function of the detector size (expressed in  $\text{mm}^2$ ) for three different source to detector distances of 2, 5 and 15 mm, respectively. The advantages of choosing a large diameter detector is readily seen. In order to maintain good resolution and high efficiency (and thus a small SMDA) the source diameter should not exceed the detector diameter.

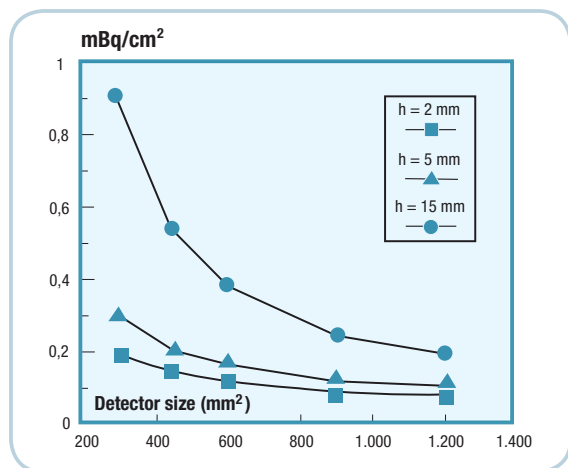


**Figure 9**  
Specific minimum detectable activity as a function of detector size for three different values of source-detector distance  $h$ .

### For Multiple Radionuclide Samples

The background in practical applications is often compromised by the presence of higher energy Alpha lines which produce counts in the spectrum at lower energies.

Alpha PIPS detectors are notably free of these tailing effects in comparison to SSB detectors of equivalent size in part because of their thin entrance window.

Comparisons between the two types of detectors have shown a difference of as much as a factor of three in this background tailing or continuum. This translates into an improvement in MDA with a factor of 3 or 1.7 for the Alpha PIPS detectors.

### The critical level

The MDA and the SMDA discussed so far are the *a priori* minimum detectable activities. In order to decide after the completion of the measurement, whether a peak has been actually observed or not, the critical level should be considered<sup>6</sup>:

$$L_c = 2.33 \sqrt{b}$$

where  $b$  = background counts.

Two cases are possible:

$S \geq L_c$ : The peak has been observed and its intensity  $I$  is given by:

$$I = S \pm k \sqrt{T + b}$$

where  $S = T - b$  represents the signal (total counts  $T$  minus background).

For a 95% confidence limit,  $k = 1.96$ .

$S < L_c$ : The peak has not been observed

and an upper limit should be stated:

$$I < + k' \sqrt{T + b}$$

For a 95% confidence limit  $k' = 1.645$ .

### Conclusions

Alpha PIPS detectors distinguish themselves from other detector types (such as SSB and diffused junction detectors) not only by their extremely rugged nature (cleanability) but also by their very thin entrance windows which result in excellent resolution, high efficiency and low detection limits.

### References

1. I.R. Williams, Nucl. Instr. Meth. 44, 160 (1966).  
R. Carchon, E. Van Camp, G. Knuyt, R. Van De Vijver, J. Devos and H. Ferdinande, Nucl. Instr. Meth. 128, 195 (1975).
2. R. Gardner, K. Verghese and H.M. Lee, Nucl. Instr. Meth. 176, 615 (1980).
3. Experimental Evaluation of the Characteristic Features of Passivated Ion Implanted and Surface Barrier Detectors for Alpha Spectrometry of Plutonium. S.K. Aggarwal, R.K. Duggal, P.M. Shah, R. Rao, H.C. Jain, Journal of Radioanalytical and Nuclear Chemistry, 120, 29 (1988).
4. P. Burger, K. De Backer, W. Schoenmaeckers, 2nd International Technical Symposium on Optical and Electro-optical Science and Engineering, 25-29 Nov., and 2-6 Dec., 1985, Cannes, France.
5. Sources and Prevention of Recoil Contaminations of Solid State Alpha Detectors C.W. Sill, D.G. Olson, An. Chem., 42, 1596 (1970).
6. L.A. Currie, An. Chem. 40, 587 (1968).
7. Handbook of Radiological Health, US Department of Health, Education and Welfare, Bureau of Radiological Health, Rockville, Maryland 20852 (1970).
8. W. Seelman-Eggebert, G. Pfenning, H. Münzel, H. Klewe-Nebenius, "Chart of the Nuclides", KFKKarlsruhe, Gersbach u. Sohn Verlag, München (1981).
9. Radiation Detection and Measurement, Fourth Edition G.F. Knoll (Univ. of Michigan, Ann Arbor) September 2010.

## Appendix 1

### Alpha Emitters by Increasing Energy<sup>7</sup>

Alpha yields are given in % of total decay. Lines marked by an \* are often used as calibration lines<sup>8</sup>, while lines underlined represent the most intense a-line of a given radioisotope.

Energy (MeV)	Radioisotope	Half-life	Yield (%)	Energy (MeV)	Radioisotope	Half-life	Yield (%)
1.83	Nd-144	2.4x10 <sup>15</sup> y	100	4.770	Np-237	2.14x10 <sup>6</sup> y	19
2.14	Gd-152	1.1x10 <sup>14</sup> y	100	<u>4.775</u>	<u>U-234*</u>	2.47x10 <sup>5</sup> y	72
<u>2.234</u>	<u>Sm-147*</u>	1.05x10 <sup>11</sup> y	100	4.778	U-233	1.62x10 <sup>5</sup> y	15
2.46	Sm-146	7x10 <sup>7</sup> y	100	<u>4.784</u>	<u>Ra-226*</u>	1602 y	95
2.50	Hf-174	2x10 <sup>15</sup> y	100	4.787	Np-237	2.14x10 <sup>6</sup> y	51
2.73	Gd-150	2.1x10 <sup>6</sup> y	100	4.811	Th-229	7340 y	11
<u>3.183</u>	<u>Gd-148*</u>	84 y	100	4.821	U-233	1.62x10 <sup>5</sup> y	83
3.18	Pt-190	6x10 <sup>11</sup> y	100	4.842	Th-229	7340 y	58
3.954	Th-232*	1.41x10 <sup>10</sup> y	23	4.863	Pu-242	3.79x10 <sup>5</sup> y	24
<u>4.013</u>	<u>Th-232*</u>	1.41x10 <sup>10</sup> y	77	4.896	Pu-241	13.2 y	0.002
4.150	U-238*	4.51x10 <sup>9</sup> y	23	4.899	Th-229	7340 y	11
<u>4.197</u>	<u>U-238*</u>	4.51x10 <sup>9</sup> y	77	4.903	Pu-242	3.79x10 <sup>5</sup> y	76
4.368	U-235*	7.1x10 <sup>8</sup> y	18	4.92	Bi-210m	3x10 <sup>6</sup> y	36
<u>4.400</u>	<u>U-235*</u>	7.1x10 <sup>8</sup> y	57	<u>4.954</u>	<u>Ac-227*</u>	21.6 y	1.2
4.415	U-235	7.1x10 <sup>8</sup> y	4	4.952	Pa-231	3.25x10 <sup>4</sup> y	22
4.445	U-236*	2.39x10 <sup>7</sup> y	26	4.96	Bi-210m	3x10 <sup>6</sup> y	58
<u>4.494</u>	<u>U-236*</u>	2.39x10 <sup>7</sup> y	74	4.967	Th-229	7340 y	6
4.556	U-235	7.1x10 <sup>8</sup> y	4	<u>5.014</u>	<u>Pa-231*</u>	3.25x10 <sup>4</sup> y	24
4.57	Bi-210m	3x10 y	6	5.028	Pa-231*	3.25x10 <sup>4</sup> y	23
4.597	U-235	7.1x10 <sup>8</sup> y	5	5.054	Th-229	7340 y	7
4.600	Ra-226*	1602 y	6	5.058	Pa-231	3.25x10 <sup>4</sup> y	11
4.621	Th-230*	8.0x10 <sup>4</sup> y	24	5.105	Pu-239*	24,400 y	12
<u>4.688</u>	<u>Th-230*</u>	8.0x10 <sup>4</sup> y	76	5.124	Pu-240*	6580 y	24
4.722	U-234	2.47x10 <sup>5</sup> y	28	<u>5.144</u>	<u>Pu-239*</u>	24,400 y	15
4.733	Pa-231	3.25x10 <sup>4</sup> y	11	5.157	Pu-239*	24,400 y	73
4.765	Np-237	2.14x10 <sup>6</sup> y	17	<u>5.168</u>	<u>Pu-240*</u>	6580 y	76

Energy (MeV)	Radio-isotope	Half-life	Yield (%)	Energy (MeV)	Radio-isotope	Half-life	Yield (%)	Energy (MeV)	Radio-isotope	Half-life	Yield (%)
5.234	Am-243	7.95x10 <sup>3</sup> y	11	5.742	Cm-243	32 y	12	6.278	Bi-211	2.15 m	16
5.267	U-232	72 y	32	5.745	Ra-223	11.43 d	9	6.28	At-219	0.9 m	97
<u>5.275</u>	<u>Am-243*</u>	7.95x10 <sup>3</sup> y	88	5.757	Th-227*	18.2 d	20	<u>6.288</u>	<u>Rn-220*</u>	55 s	100
<u>5.304</u>	<u>Po-210*</u>	138.4 d	100	5.763	Cm-244	17.6 y	23	6.34	Th-226	30.9 m	79
5.304	Cm-245*	9.3x10 <sup>3</sup> y	7	5.786	Cm-243	32 y	73	6.340	Fr-221	4.8 m	82
5.324	U-232	72 y	68	5.79	Ac-225	10.0 d	28	6.424	Rn-219	4.0 s	90
5.342	Cm-246	5.5x10 <sup>3</sup> y	19	5.806	Cm-244	17.6 y	77	6.437	Es-254	276 d	6
5.340	Th-228*	1.910 y	28	5.812	Cf-249	360 y	84	6.551	Rn-219	4.0 s	94
<u>5.362</u>	<u>Cm-245*</u>	9.3x10 <sup>3</sup> y	80	5.816	U-230	20.8 d	32	6.56	Ra-222	38 s	100
5.386	Cm-246	5.5x10 <sup>3</sup> y	81	5.83	Ac-225	10.0 d	54	<u>6.623</u>	<u>Bi-211*</u>	2.15 m	81
5.42	Bk-249	314 d	0.0015	<u>5.851</u>	<u>Cf-251*</u>	800 y	45	6.640	Es-253	20.47 d	93
<u>5.423</u>	<u>Th-228*</u>	1.910 y	71	5.868	At-211	7.21 h	41	6.65	At-218	2 s	6
5.443	Am-241	458 y	13	5.87	Bi-213	47 m	2	<u>6.694</u>	<u>At-218*</u>	2 s	90
5.447	Ra-224	3.64 y	6	5.887	U-230	20.8 d	68	6.777	Po-216	0.15 s	14
5.448	Bi-214	19.7 m	0.012	5.977	Th-227*	18.2 d	23	<u>6.819</u>	<u>Rn-219*</u>	4.0 s	85
5.456	Pu-238*	86	28	5.987	Cf-250	13 y	17	7.027	Fm-255	20.1 h	91
<u>5.486</u>	<u>Am-241*</u>	458 y	86	5.994	Cm-243	32 y	6	7.07	At-217	32 ms	100
5.490	Rn-222	3.823 d	100	<u>6.002</u>	<u>Po-218*</u>	3.05 m	100	7.14	Rn-218	35 ms	99
<u>5.499</u>	<u>Pu-238*</u>	86 y	72	6.031	Cf-250*	13 y	83	7.145	Fm-254	3.24 h	14
5.512	Bi-214	19.7 m	0.008	<u>6.038</u>	<u>Th-227*</u>	18.2 d	24	7.187	Fm-254	3.24 h	85
5.52	Bk-247	1.4x10 <sup>3</sup> y	58	<u>6.051</u>	<u>Bi-212*</u>	60.6 m	25	7.28	Po-211m	25 s	100
5.537	Ra-223	11.43 d	9	6.061	Cm-243	32 y	6	<u>7.386</u>	<u>Po-215*</u>	1.78 ms	7
5.607	Ra-223*	11.43 d	26	6.071	Cm-242	163 d	26	<u>7.450</u>	<u>Po-211*</u>	0.52 s	97
5.666	Cf-251	800 y	55	6.076	Cf-252	2.65 y	15	<u>7.687</u>	<u>Po-214*</u>	164 μs	100
5.68	Bk-247	1.4x10 <sup>3</sup> y	37	6.090	Bi-212*	60.6 m	10	<u>8.376</u>	<u>Po-213*</u>	4.2 μs	99
<u>5.685</u>	<u>Ra-224*</u>	3.64 d	94	6.115	Cm-242	163 d	74	<u>8.784</u>	<u>Po-212*</u>	0.30 μs	97
5.707	Th-227	18.2 d	8	<u>6.118</u>	<u>Cf-252*</u>	2.65 y	84	8.88	Po-211m	25 s	7
<u>5.716</u>	<u>Ra-223*</u>	11.43 d	54	6.126	Fr-221	4.8 m	15	11.65	Po-212m	45 s	97
5.73	Ac-225	10.0 d	10	6.22	Th-226	30.9 m	19				

www.mirion.com

Copyright ©2018 Mirion Technologies, Inc. or its affiliates. All rights reserved. Mirion, the Mirion logo, Canberra, PIPS and other trade names of Mirion products listed herein are trademarks and/or registered trademarks of Mirion Technologies, Inc. and/or its affiliates in the United States and/or other countries.

Third party trademarks mentioned are the property of their respective owners.



C39168 - 12/2011